Systems analysis of miR-199a/b-5p and multiple miR-199a/b-5p targets during chondrogenesis

Patel K[1]*, Barter MJ[2]*, Soul J[2], Proctor CJ[1], Clark IM[3], Young DA[2], Shanley DP[1]

[1]Campus for Ageing and Vitality, Biosciences Institute, Newcastle University, Newcastle upon-Tyne, NE4 5PL, UK.

[2]Regenerative Medicine, Stem Cells, Transplantation, Biosciences Institute, Newcastle University, Newcastle, upon, UK Tyne, NE1 4EP.

[3]School of Biological Sciences, University of East Anglia, Norwich, NR4 7TJ, UK.

*****Authors contributes equally.

ABSTRACT

Changes chondrocyte gene expression can contribute to the development of osteoarthritis (OA), and so better understanding of the regulative processes during chondrogenesis can highlight potential drug targets for OA. microRNAs (miRNAs) have been a focus of chondrogenesis/ OA research and we have used a combined experimental, bioinformatic, and systems biology approach to explore multiple miRNA-mRNA interactions that regulate chondrogenesis. We identified paralogues miR-199a-5p and miR-199b-5p as pro-chondrogenic regulators of chondrogenesis through bioinformatic analysis. Experimental work demonstrated alteration of miR-199a-5p or miR-199b-5p expression led to significant inverse modulations of chondrogenic biomarkers: *ACAN*, *COL2A1*, *SOX9* and glycosaminoglycan levels. Potential miR-199a/b-5p targets were then identified using RNAseq combined with bioinformatic analysis to identify *FZD6*, *ITGA3* and *CAV1* as highly likely candidates. Through knockdown experiments we indicated a strong antagonistic relationship between miR-199a/b-5p and *FZD6*, *ITGA3* and *CAV1*. Luciferase assays using *FZD6* and *ITGA3* 3'UTRs luciferase assays indicated both mRNAs to be targets of *miR-199a-5p.* The experimental work was used to generate and parameterize a multi-miRNA 14-day chondrogenesis kinetic model to be used as a repository for the experimental work and as a resource for further investigation of this system. This is the first multi-miRNA model of any system, and it highlights that many other miRNAs may be involved in the regulation of this system and was used to predict experimental gaps not covered by experimental work.

Keywords: microRNA, chondrogenesis, systems biology, RNA-seq, bioinformatics

Introduction:

Differentiation of mesenchymal stem cells (MSCs) into chondrocytes is known as chondrogenesis[1]. This is an important process during development, as is a pre-requisite for skeletogenesis to occur. Chondrocytes perform the vital roles of generating and maintaining cartilage during embryogenesis, but also within adults' chondrocytes are found in many tissues including the trachea, ribs, nose and at ends of joints (known as articular cartilage) [2]. The master transcription factor responsible for triggering chondrogenesis is SOX9 and during this process chondrocytes secrete anabolic proteins such as Collagen Type II and aggrecan, which are respectively encoded by their protein sub-units COL2A1 and ACAN, and these fibres constitute a significant functional portion of cartilaginous extracellular matrix (ECM) [2,3]. Over time and influenced by a mixture of factors such as age, epigenetics and mechanical stress, chondrocytes will increasingly express catabolic proteins such as MMP13 and ADAMTS5 which respectively degrade COL2A1 and ACAN [3]. During skeletogenesis, the process known as endochondral ossification chondrocytes will naturally become hypertrophic and differentiate into osteoblasts for healthy bone growth. However, when chondrocytes within articular cartilage become hypertrophic, this leads to detrimental effects, as the cartilage maintenance is greatly diminished, leading to stiffer, less resilient, and joints less able to bear force. Ultimately the chronic loss of cartilage contributes to the extremely debilitating condition known as OA, which has few treatment options, such as pain relief drugs or surgery, and no cure [4,5]. Research into the regulation of chondrogenesis could identify regulatory processes and potential drug targets for OA for pain relief or to delay the progress of hypertrophy. Numerous studies have identified significantly altered microRNAs (miRNAs) during chondrogenesis, which includes investigation into the two important chondrocyte selective miRNAs, miR-140 and miR-455 [6].

miRNAs are short non-coding RNAs - roughly 19-22nt long, that negatively regulate

target mRNAs [7,8]. Mammalian miRNA-mRNA interactions occur via complementary sequence specificity between a 7-8nt stretch of the miRNA known as the seed sequence, and positions along the 3'UTR of the target mRNA [9,10]. miRNA-mRNA interactions are complex because a single mRNA can be targeted by many miRNAs, and a single miRNA can target many mRNAs. The complexity of miRNA-mRNA interactions led us to perform a combined bioinformatic, experimental and systems biology approach to better understand the relationship between microRNAs which may be important to chondrogenesis, and their predicted targets. We identified miR-199a-5p and miR-199b-5p as pro-chondrogenic miRNAs. Just as with miR-140-5p and miR-455, we anticipated miR-199a-5p and miR-199b-5p (miR-199a/b-5p) to target multiple mRNAs. To this end we used experimental, informatic and literary data to build a gene regulatory network (GRN) to explain how mir-199a/b-5p regulate chondrogenesis. The GRN included three targets identified through RNAseq analysis (*FZD6*, *ITGA3* and *CAV1*). Kinetic models were built from the GRN by using experimental data to inform model parameters and we used the model to create simulations to fill experimental knowledge gaps.

Results:

Analysis with *TimiRGeN* identified *miR-199b-5p* to be upregulated during chondrogenesis

Our previously generated 14-day chondrogenesis time series dataset was analysed with the *TimiRGeN R* package - a novel *Bioconductor* tool we previously developed to analyse longitudinal miRNA-mRNA expression datasets [6,11]. Prior to using *TimiRGeN*, the transcriptomic data underwent timepoint based differential expression analysis, using the 0 time-point as the control group for samples at days: 1, 3, 6, 10, 14, and thus created differential expression data for five time-points. *TimiRGeN* identified signalling pathways of interest over the 14-day time series data (Table 1) Eight signalling pathways were enriched in at least three of the five time points (Figure 1). The *TimiRGeN* pipeline was then used to predict miRNA-mRNA interactions that may regulate each of the eight pathways. miRNA-mRNA interactions were kept if the miRNA and mRNA involved in the interaction has a Pearson correlation <-0.75 and if the interaction was predicted in at least two of the following three databases: TargetScan, miRDB or miRTarBase [12–14]. To identify which miRNAs involved in the miRNA-mRNA interactions were positively changing in each of the eight signalling pathways we scaled the Log2FC values from *DESeq2*. The genes (mRNAs and miRNAs) from each pathway which had a scaled Log2FC value above 1 at any point of the time course was highlighted (Figure 1).

hsa-miR-140-5p was the most positively changing miRNA in the following seven pathways: Adipogenesis, Clear cell renal cell carcinoma pathways, Epidermal growth factor/Epidermal growth factor receptor, Endochondral ossification, Endochondral ossification with Skeletal Dysplasia, Gastrin signalling pathway and Vascular endothelial growth factor-A/Vascular endothelial growth factor receptor 2 signalling pathway, while *hsa-miR-199b-5p* was the second most positively changing gene in the following six pathways: Clear cell renal cell carcinoma pathways, Epidermal growth

factor/Epidermal growth factor receptor, Endochondral ossification, Endochondral ossification with Skeletal Dysplasia, Gastrin signalling pathway and Vascular endothelial growth factor-A/Vascular endothelial growth factor receptor 2 signalling pathway. Other genes such as hsa-miR-455-5p and *BMP2* were also of interest, but we focused on hsa-miR-199b-5p since it is comparatively under-researched within the context of chondrogenesis. Furthermore, our previous work identified miR-199b-5p and its paralogue miR-199a-5p as significantly upregulated during chondrogenesis, therefore we chose to focus on both paralogues of miR-199-5p within the context of chondrogenesis [6].

Wikipathways	D1	D2	D3	D10	D14
Adipogenesis	X	X	X		
Apoptosis-related network due to altered Notch3 in ovarian cancer					X
Burn wound healing		X			
Clear cell renal cell carcinoma pathways		X	X	X	
EGF/ EGFR signaling pathway		X	X	X	X
Endochondral ossification		X	X	X	X
Endochondral ossification with skeletal dysplasias	X	X	X	X	X
Focal adhesion				X	X
Focal adhesion: PI3K-Akt-mTOR-signaling pathway				X	
Gastrin Signaling pathway	X	X			X
Hepatitis C and hepatocellular carcinoma			X		
Malignant pleural mesothelioma				X	
Mir-509-3p alteration of YAP1/ ECM axis			X		
Metabolic reprogramming in colon cancer	X	X		X	
Oscantin M signaling pathway					X
PDGF pathway					X
Retinoblastoma gene in cancer			X		
Spinal cord injury	X				
TGF-beta receptor signaling	X				
TGF-beta receptor signaling in skeletal dysplasias	X				
TGF-beta receptor signaling pathway	X				X
Type I collagen synthesis in the context of osteogenesis imperfecta		X	X		
VEGFA-VEGFR2 signaling pathway	X	X	X	X	X

Table 1. The 10 most enriched signalling pathways for each time point based differential expression analyses conducted (DX/ D0) (D=day, D1, D3, D7, D10, D14) are presented. An X marks if the mechanistic pathway was significantly enriched (Benjamini-Hochberg adjusted P value < 0.05) at a that time point.

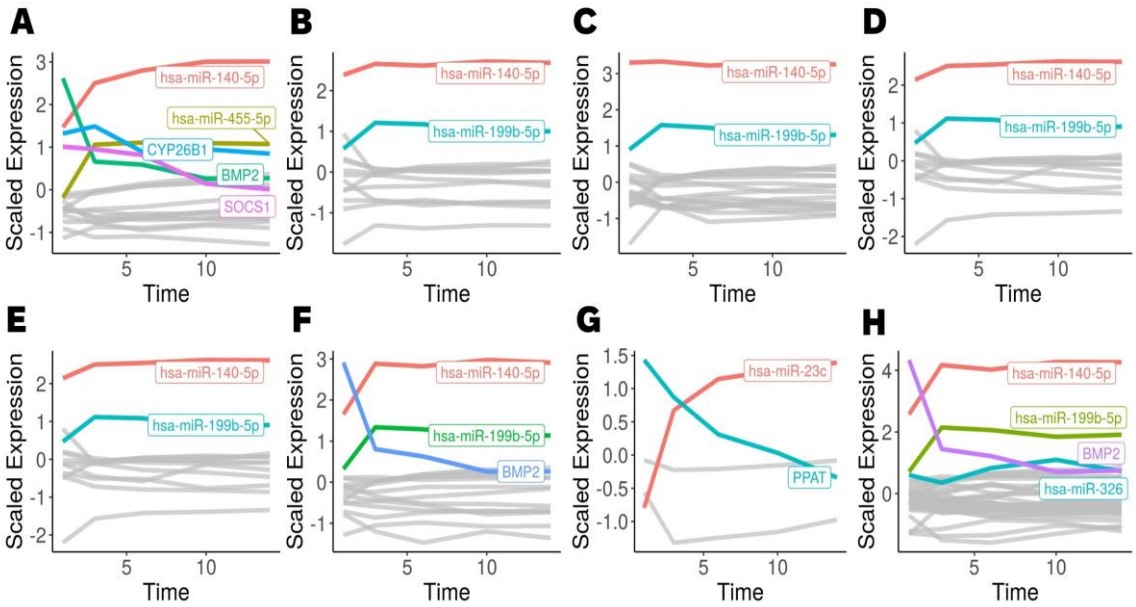

Figure 1. Line plots displaying scaled log2fc values over the 14-day time course. Eight pathways of interest were explored here: A) Adipogenesis, B) Clear cell renal cell carcinoma pathways, C) Epidermal growth factor/Epidermal growth factor receptor signalling pathway, D) Endochondral ossification, E) Endochondral ossification with skeletal dysplasia's, F) Gastrin signalling pathway, G) Metabolic reprogramming in colon cancer, and H) Vascular endothelial growth factor A/ Vascular endothelial growth factor receptor 2 signalling pathway. Here, individual genes found in the filtered miRNA-mRNA interactions for each pathway are plotted along a time course. Only genes (miRNAs or mRNAs) that have a scaled log2FC value of at least 1 at any point of the line plot are highlighted and labelled.

Expression of chondrogenic biomarkers and glycosaminoglycan levels change over time after altering miR-199a-5p or miR-199b-5p expression.

To identify if miR-199a-5p and miR-199b-5p regulate chondrogenesis we performed MSC chondrogenic differentiation and measured the consequences of miR-199a-5p overexpression on chondrogenic biomarkers *ACAN*, *COL2A1 and SOX9* by qPCR experiments and GAG (glycosaminoglycan) levels biochemically. Significant upregulation was seen in *ACAN*, *COL2A1* and GAG levels (Figure 2A). In contrast, when miR-199b-5p expression was inhibited *ACAN*, *COL2A1* and *SOX9* were taken at were significantly downregulated at multiple time points, especially those early during chondrogenesis. GAG levels were also significantly decreased, by ~60%, at day 7 (Figure 2B). Our results indicated both miR-199a-5p and miR-199b-5p contributed towards positive regulatory roles during chondrogenesis.

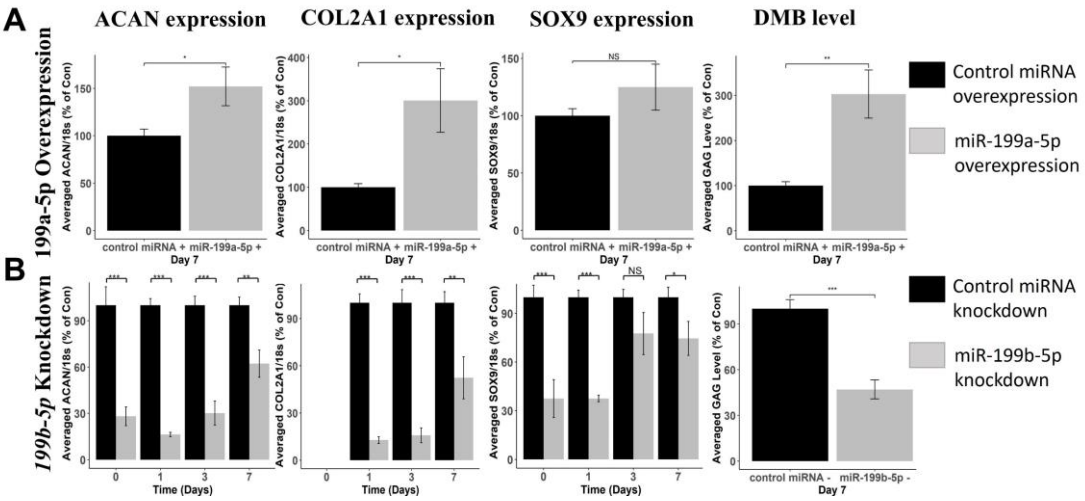

Figure 2. Chondrocytes were transfected for 24 hours with a non-target miRNA control, miR-199a-5p mimic or miR-199b-5p hairpin inhibitor. **A)** miR-199a-5p was overexpressed in chondrocytes and measured at day 7 of chondrogenesis. Measurements of chondrogenic biomarkers were taken from three human MSC donors, and technical repeats of each were carried out in quadruple. Averaged qPCR values are plotted along with the standard error of the mean values (SEM), where the control level set at 100%. DMB measurements were taken at day 7 to determine GAG levels**. B)** miR-199b-5p was inhibited prior to chondrogenesis initiation, after initiation measurements of *ACAN*, *COL2A1* and *SOX9* were taken at days: 0, 1, 3 and 7 of chondrogenesis, and DMB measurements were taken at day 7 to determine GAG levels. qPCR results for day 0 were undetectable for *COL2A1*. Percentages were calculated from the means of qPCR data with the control levels at each day termed 100% to allow visualisation. NS = not significant, * = <0.05, ** = < 0.01, *** = < 0.001. Samples numbers are as per **A**.

***FZD6, ITGA3* and *CAV1* were the most significantly upregulated *miR-199a/b-5p* targets in MSCs during chondrogenesis.** Multiple mRNA targets of miR-199a/b-5p are likely regulated during chondrogenesis. To elucidate those most affected by miR-199 modulate we performed an RNAseq experiment to identify candidate targets during the early phase of MSC chondrogenesis comparing MSC samples which were undifferentiated (day 0) and MSC samples which were in the early stages of chondrogenesis (day 1). We chose to inhibit miR-199a-5p or miR-199b-5p since supraphysiological overexpression of miRNA mimics can lead to spurious findings [15]. Undifferentiated control MSC samples were contrasted with against undifferentiated MSCs with either miR-199a-5p or miR-199b-5p inhibition, which respectively resulted in 87 and 46 significantly differentially expressed genes (adjusted P values < 0.05). Similar comparisons at day 1 of chondrogenesis revealed inhibition of miR-199a-5p or miR-199b-5p respectively resulted in 674 and 817 differentially expressed genes. 25 and 341 genes intersected between day 0 and day 1 chondrogenesis inhibition experiments, indicating that both microRNAs may share functional repertoire of targets. Contrasting the day 1 chondrogenesis control samples over the day 0 control samples lead to 4391 upregulated and 4168 downregulated significantly differentially expressed genes (< 0.05 adjusted p value). Positively changing genes included well studied pro-chondrogenic markers such as COL2A1 (log2fc =11.6), ACAN (log2fc = 9.18) and SOX9 (log2fc = 3.37). Putting the hundred most significantly differentially expressed genes (Supplementary Table 3) through enrichr analysis found the most likely cell type to be chondrocytes according to the Panglao database. Gene Ontology (GO) term analysis confirmed that the cells were differentiating towards chondrocytes with terms such as extracellular matrix organization and collagen-containing extracellular matrix significantly (adjusted P values < 0.05) enriched. The knockdown experiments showed that well known chondrogenesis genes such as COL2A1, ACAN and SOX9 were significantly downregulated in day one samples, when contrasted to day controls, which strongly indicates the progression to chondrogenesis has been hindered by miR-199a-

5p and miR-199b-5p inhibition.

Gene Ontology (GO) term analysis was conducted to identify biological processes linked to miR-199a/b-5p inhibition (Figure 3A). Interestingly several gene sets associated with chondrogenesis were suppressed/ less activated during day 1 analyses, including: extracellular matrix constituents, skeletal system morphogenesis, extracellular matrix and collagen containing extracellular matrix. The significantly differentially expressed genes were further analysed using the *miRNAtap R* package to predict *miR-199a-5p* and *miR-199b-5p* targets[16]. miRNAtap scored each predicted miRNA-mRNA interaction recorded for *miR-199a-5p* and *miR-199b-5p* from five popular miRNA prediction tools (e.g. TargetScans) to rank the most likely targets. Twenty-one potential mRNA targets were predicted to be targeted by both miRNAs: *ABHD17C, ATP13A2, CAV1, CTSL, DDR1, FZD6, GIT1, HIF1A, HK2, HSPA5, ITGA3, M6PR, MYH9, NECTIN2, NINL, PDE4D, PLXND1, PXN, SLC35A3, SLC35D1* and *VPS26A*. Of the 21 targets, *FZD6* and *NINL* were the only predicted target genes found to be significantly differentially expressed in the MSCs pre-differentiation (day 0) following miR-199a-5p or miR-199b-5p inhibition.

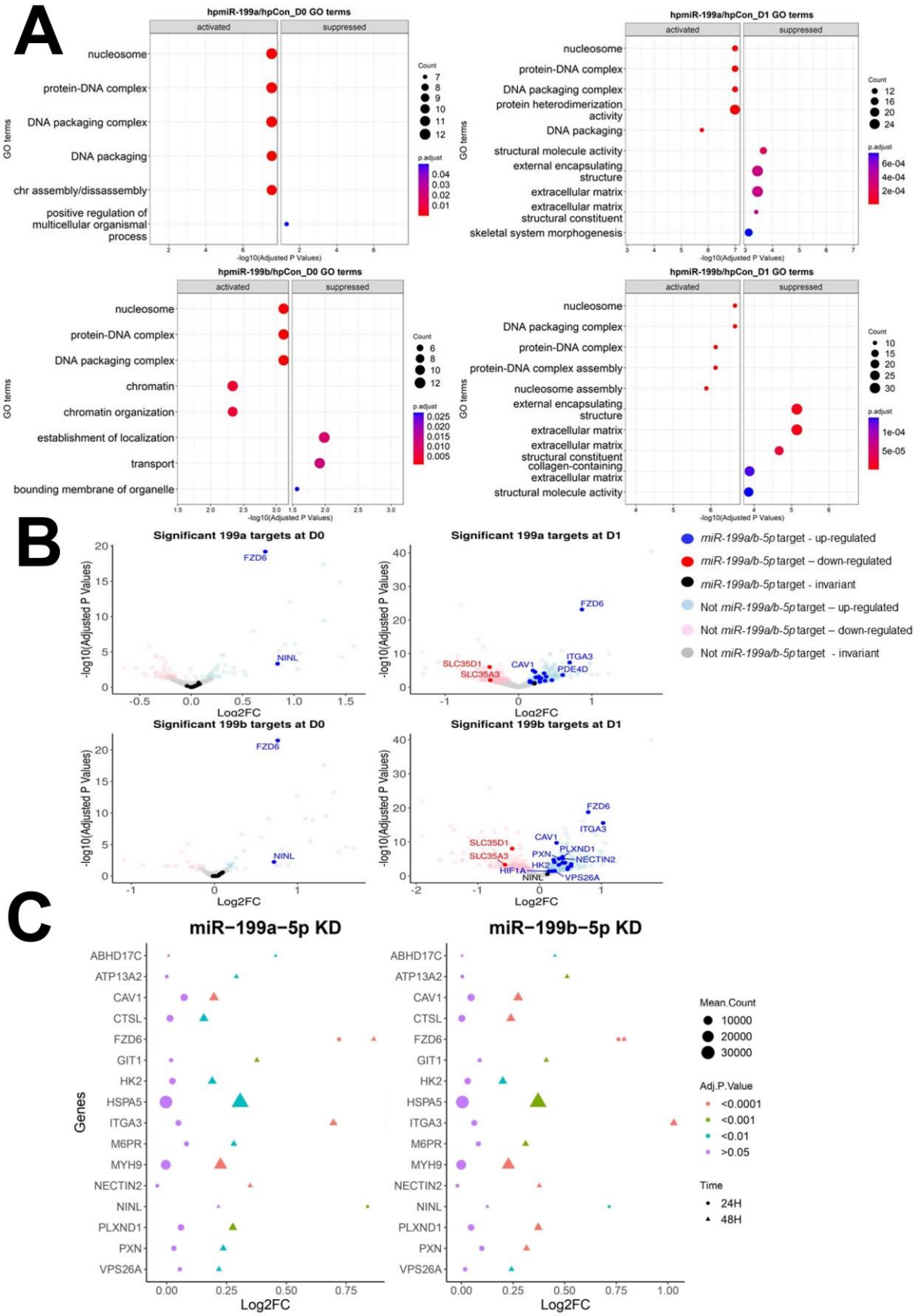
A
hpmiR-199a/hpCon_D0 GO terms
activated
suppressed
nucleosome
protein-DNA complex
DNA packaging complex
DNA packaging
chr assembly/dissassembly
positive regulation of multicellular organismal process
GO terms
-log10(Adjusted P Values)
Count
p.adjust
hpmiR-199a/hpCon_D1 GO terms
nucleosome
protein-DNA complex
DNA packaging complex
protein heterodimerization activity
DNA packaging
structural molecule activity
external encapsulating structure
extracellular matrix
extracellular matrix structural constituent
skeletal system morphogenesis
hpmiR-199b/hpCon_D0 GO terms
nucleosome
protein-DNA complex
DNA packaging complex
chromatin
chromatin organization
establishment of localization
transport
bounding membrane of organelle
hpmiR-199b/hpCon_D1 GO terms
nucleosome
DNA packaging complex
protein-DNA complex
protein-DNA complex assembly
nucleosome assembly
external encapsulating structure
extracellular matrix
extracellular matrix structural constituent
collagen-containing extracellular matrix
structural molecule activity
B
Significant 199a targets at D0
Significant 199a targets at D1
Significant 199b targets at D0
Significant 199b targets at D1
-log10(Adjusted P Values)
Log2FC
FZD6
NINL
SLC35D1
SLC35A3
CAV1
ITGA3
PDE4D
PLXND1
NECTIN2
PXN
HK2
HIF1A
VPS26A
miR-199a/b-5p target - up-regulated
miR-199a/b-5p target – down-regulated
miR-199a/b-5p target - invariant
Not miR-199a/b-5p target – up-regulated
Not miR-199a/b-5p target – down-regulated
Not miR-199a/b-5p target - invariant
C
miR−199a−5p KD
miR−199b−5p KD
Genes
ABHD17C
ATP13A2
CAV1
CTSL
FZD6
GIT1
HK2
HSPA5
ITGA3
M6PR
MYH9
NECTIN2
NINL
PLXND1
PXN
VPS26A
Log2FC
Mean.Count
Adj.P.Value
<0.0001
<0.001
<0.01
>0.05
Time
24H
48H

Figure 3. Results from RNAseq analysis of control miRNA, *miR-199a-5p* and *miR-199b-5p* knockdown experiments. **A)** Gene Set Enrichment Analysis (GSEA) was used to conduct Gene ontology (GO) analysis for the significantly differentially expressed genes found from miR-199a-5p or miR-199b-5p inhibition at day 0 and day 1 of chondrogenesis. Up to five activated and five suppressed pathways are displayed for each DE analysis. All GO terms shown have an adjusted P value of <0.05. Count size represents the genes found in a pathway and this determined the size of the circles. **B)** Volcano plots with the *miRNAtap*-selected 21 *miR-199a/b-5p* targets highlighted and if space on the plot is available labelled. Up-regulated targets are blue, down-regulated targets are red and invariant targets are black. Non-*miR-199a/b-5p* target genes were also displayed, and of these up-regulated genes are pink, down-regulated genes are light blue and non-significantly differentially expressed genes are light grey. The cut-off for significance was an adjusted (BH) P value <0.05. **C)** More detailed account of the 21 miR-199a/b-5p targets found from RNAseq experiment.

To examine the expression patterns of the 21 genes found through our bioinformatic analysis (Figure 3C), the genes were also explored in our microarray study (Supplementary Table 2) [6]. In addition, we used *SkeletalVis* to contrast the behaviour of the 21 genes in other MSC derived chondrogenesis studies (Supplementary Table 3) [17–19]. The tables showed many of genes found through our bioinformatic analysis to be significantly downregulated during chondrogenesis in multiple studies, and this included *CAV1*, *FZD6*, *ITGA3*, and *MYH9*. We decided to further explore if *FZD6*, *ITGA3* and *CAV1* were true targets of miR-199a/b-5p. Interestingly, *FZD6* and *NINL* were the only genes significantly upregulated during miR-199a/b-5p inhibition at day 0, but *NINL* was not further explored as they were not significantly upregulated at day 1 following miR-199a/b-5p inhibition.

miR-199a/b-5p targets were upregulated during miR-199a/b-5p inhibition

To test the effects miR-199a-5p and miR-199b-5p had on the predicted targets that were identified through RNAseq, we performed a series of inhibition experiments. Since the miRNAs shared the same seed site sequence (nucleotides 2-8; 5'-CCAGUGUU-3'), we wanted to evaluate if knockdown of one of the miRNAs would affect expression of the other paralogue. We performed miR-199b-5p knockdown on MSCs undergoing chondrogenesis and measured miR-199a/b-5p levels over 7 days (Figure 4A). We did see non-detectable levels of miR-199a/b-5p during the 7-day time course, indicating knockdown of one miRNA may have also affected the other miRNA. To further check this, we wanted to see if knock-down of one miRNA would lead to similar or different effects to knock-down of both miRNAs. For this, we picked to supress expression of miR-199a-5p as it was the more highly expressed of the two paralogues and contrasted it to inhibition of miR-199a/b-5p. We tested the effects of the knockdowns by measuring the expression of the two most significantly enriched predicted miR-199a/b-5p targets from our bioinformatic analysis – *FZD6* and *ITGA3*. We saw significant

enrichment of *FZD6* and *ITGA3*, however we generally saw a greater enrichment from miR-199a-5p knock-down, in contrast to miR-199a/b-5p knock-down – though none of the differences between treatments were statistically significant. We also tested how *CAV1* expression changed after miR-199b-5p inhibition over the same time course, and we saw *CAV1* levels to become significantly enriched post miR-199b-5p inhibition. Unlike FZD6 and ITGA3, CAV1 has previously been established to be a direct binding partner of miR-199a-5p [20]. To identify if *FZD6* and *ITGA3* were also direct miRNA-mRNA interactions we cloned the 3' UTR regions of *FZD6* and *ITGA3* directly downstream of the firefly luciferase gene in the vector pGL3-basic which also contains a control renilla luciferase gene for transfection efficiency normalisation. These plasmids were transiently transfected into the chondrocytic cell line SW1353 along with control or *miR-199a-5p* mimics (Figure 4C). Both *FZD6* and *ITGA3* 3'UTRs reduced the firefly/renilla ratio levels when compared to the empty control vector, suggesting these contain potentially repressive elements. Indeed, the co-introduction of an excess of miR-199a-5p into the cells further repressed the 3'UTR containing vectors firefly/renilla ratio but not that of the control vector, suggesting both genes are direct miR199a-5p targets.

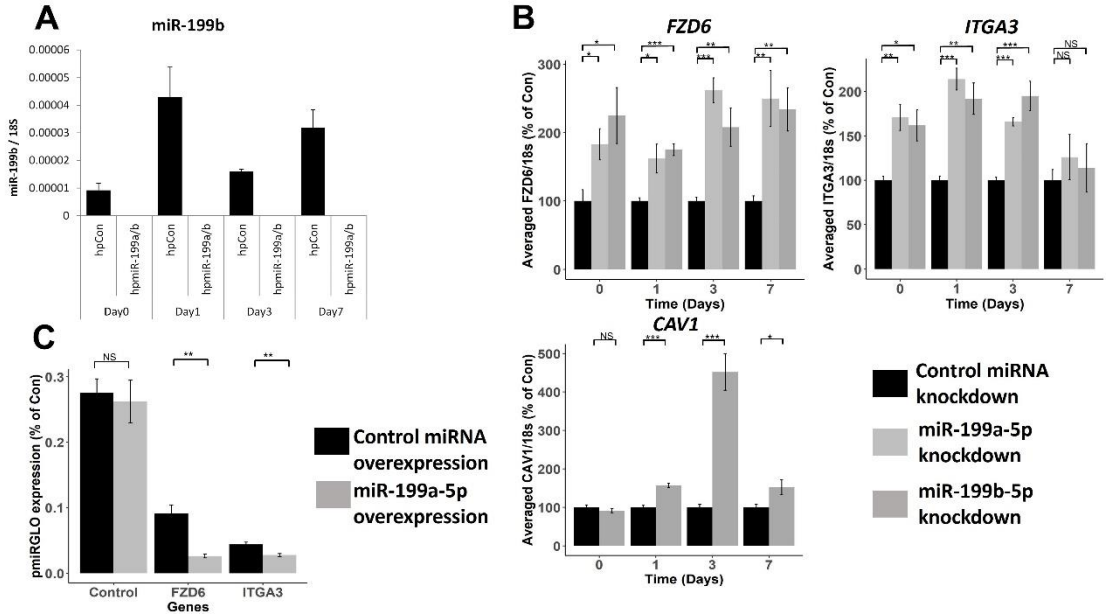

Figure 4. A) During control and miR-199a/b-5p inhibition over 7 days of chondrogenesis miR-199b-5p levels were measured to check if the knockdowns worked. **B)** MSCs were transfected with hairpins to knockdown miR-199a-5p expression, miR-199b-5p expression or miR-199a/b-5p expression. FZD6 and ITGA3 expression was measured after miR-199a-5p and miR-199a/b-5p inhibition, and CAV1 was measured after miR-199b-5p inhibition. Measurements were taken at times 0, 1, 3 and 7 days after transfection. Measured expression values were normalised using 18S as a control. **C)** Luciferase assays showing luciferase expression following co-transfection of miR-199a-5p target 3' UTR reporter constructs for 24 hours. Expression was normalised to renilla luciferase and presented as percentage of control levels. Values are the mean +/- SEM of data pooled from three independent experiments. NS = not significant, * = <0.05, ** = < 0.01, *** = < 0.001.

Kinetic modelling creates an *in silico* demonstration of how miR-199a-5p/miR-199b-5p regulates chondrogenesis

Regulation of chondrogenesis by microRNAs is complex. We attempted to capture this complexity using an In Silico model (Figure 5A). Only using the experimental data presented in this manuscript, and our previous microarray work, we developed a model to demonstrate the relationships between chondrogenic biomarkers and the targets of *miR-199a/b-5p* we identified through RNAseq and subsequent knockdown experiments. Finally, we used events to knockdown miR-199a-5p or miR-199b-5p to replicate the effect of our knockdowns (Figure 5B). The experiments shown in figures 2A, 2B and 4B were used to parameterise the model, and since the experiments were performed in a staggered manner, we can use to model to make predictions to fill experimental gaps. For example, using this model we predicted the dynamics of the chondrogenesis biomarkers and *CAV1* after miR-199a-5p knockdowns and the dynamics of *FZD6* and *ITGA3* after miR-199b-5p knockdown. Most objects within the model were based on experimental data, and the differences between the experimental data and simulated data are calculated by Mean Squared Error (MSE). Most species, have a MSE of lower than 3 during the different conditions (~84%) (3/14) indicating many of the experimental dynamics were captured by this model.

Based on our initial model, we added further detail to increase the possible predictions of our model based on data from the literature. This included the addition of Tumour Growth Factor Beta (TGFB) as a trigger for chondrogenesis initiation – as we had during our chondrogenesis MSC experiments. We found strong mechanistic links between TGFB signalling and *CAV1* expression via SRC kinase. Based on our previous work we also included miR-140-5p as it has been proven as a major regulator of chondrogenesis, and with our kinetic model we predicted how miR-199a-5p or miR-199b-5p inhibition affected miR-140-5p. Further to this, we identified several flaws in our initial model. Firstly, by simulating the miR-199a-5p and miR-199b-5p knockdown

to last until day 7 to match figure 4A, we saw that *SOX9* mRNA, *COL2A1* mRNA and *ACAN* mRNA dynamics between days 1 and 7 of miR-199b-5p knockdown was flat. Furthermore, our CAV1 dynamics were also flat during miR-199b-5p knockdown. Figure 2B shows, from miR-199b-5p knockdown, the chondrogenesis biomarkers had a sharp decrease followed by a steady rise until day 7, and in order to match the earlier effects of miR-199b-5p knockdown, we simulated the knockdown to last until day 4.5 instead of day 7. Doing so increased the similarities between our experimental data and simulations. Secondly, we wanted a more detailed model to contain other miR-199a/b-5p targets which may have been alluded to in our RNAseq experiment, but not further explored such as *MYH9, PDE4D*. We added a blackbox names 'OtherTargets' to represent other targets which miR-199a/b-5p regulate during chondrogenesis. Also, we found wanted to slow down the interactions between the miR-199a/b-5p targets and *SOX9*, and to do this we included SOX9 protein and SOX9 phospho-protein to the model. This meant the model could also predict the dynamics of different omics of SOX9 – but we lacked the data to provide any evidence for our predictions. Finally, our initial model used simplistic functions, with few parameters and we found using more detailed functions with additional parameters improved our model dynamics greatly (Supplementary Materials) (Figure 5C, Figure 5D).

From reperforming the modelling, we saw improved dynamics for several model objects e.g. GAG, *CAV1*, *SOX9*, *ACAN*, *COL2A1*. Our MSE values which were used to quantify how similar our models' simulations were in contrast to our experimental data. Generally, our MSE values were better in our enhanced model for the chondrogenesis biomarkers and GAG levels, though our MSE values were better in our initial model for the miR-199a/b-5p targets. We found that now 80% (3/15) of the MSE values were below 3, indicating our enhanced model was still able to capture more of the experimental data. Overall, we saw the dynamics improved in the enhanced model, and in addition, we could make predictions on how miR-140-5p would levels would

indirectly be influenced from knock-down of miR-199a-5p or miR-199b-5p and such a multi-miRNA model has not yet been created before. Further pathways and important genes such as the SMAD2/3 signalling pathways and the Wnt signalling pathway may also play an important role in this system but could not be explored via modelling with our current level of data. We developed a hypothesis rich GRN to display further pathways which were not in the scope of this project (Supplementary Figure 2).

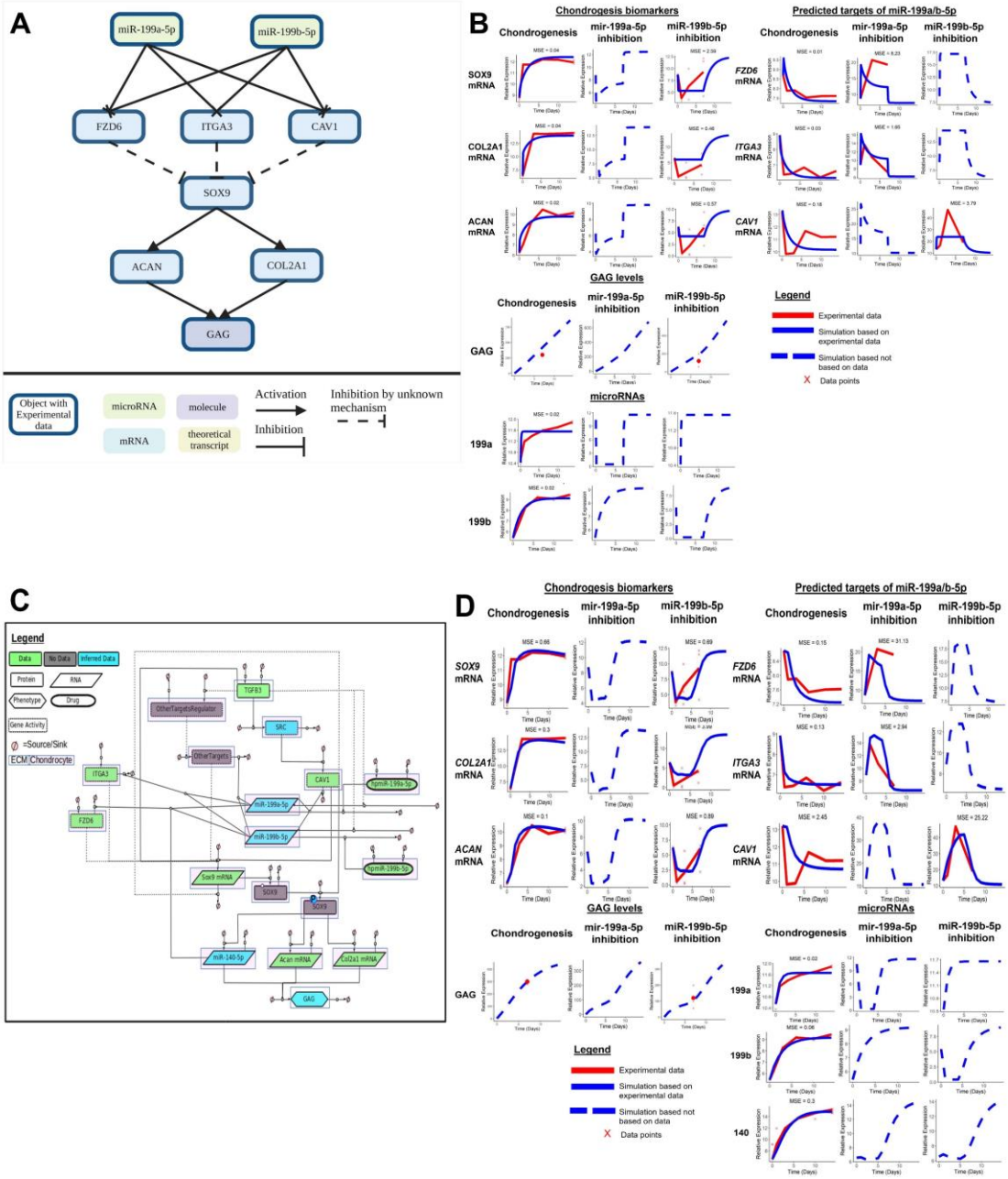

Figure 5. Initial kinetic modelling of miR-199a/b-5p regulation of chondrogenesis. A) Schematic of how miR-199a/b-5p modulation effects the predicted miR-199a/b-5p *FZD6*, *ITGA3* and *CAV1*, and the chondrogenic biomarkers *SOX9*, *COL2A1*, *ACAN* and GAG. **B)** Simulations (blue lines) from the kinetic modelling were contrasted against

the experimental data – if available (red line) and a MSE score is provided in these cases. Alternatively, if no experimental data was available, a dashed blue line displays the predicted behaviour of the gene. If multiple measurements were displayed using red crosses. **C)** A more detailed model displaying how miR-199a/b-5p regulates chondrogenesis via *FZD6*, *ITGA3* and *CAV1* mRNAs**,** in GRN form. Here information from literature was added and miR-140-5p was added to the model. The GRN shown here is a minimalistic version of Supplementary Figure 1. This was used to inform the topology of a kinetic model which aimed to explain how miR-199a-5p and miR-199b-5p act as pro-chondrogenic regulators by down-regulating activity of *FZD6*, *ITGA3* and *CAV1* mRNAs. This GRN contained 18 species including: two proteins (TGFB3, SOX9), one phospho-protein (phospho-SOX9) three mRNAs (*SOX9*, *ACAN*, *COL2A1*), three miRNAs (miR-140-5p, miR-199a-5p, miR-199b-5p), two drugs (hpmiR-199a-5p, hpmiR-199b-5p), six Gene Activity (SRC, CAV1, FZD6, ITGA3, OtherTargets, OtherTargetsRegulator), and one phenotype (GAG). Each species has a sink and a source. Species are also shaped based on their properties: Proteins are rectangles, RNAs are rhombus, Phenotypes are hexagons, Drugs are oval, Gene Activity are rectangles with dotted lines. Species are also highlighted with a white box if they are found in the ECM or pink if they are found within a chondrocyte. Edges between species are solid if there is literature/ data supporting an interaction or dotted if there the interaction is hypothetical. Species are also colour coded: green if there is associated data, blue if there is some data and the rest has been inferred based on literature, or grey if there is no data associated with the species. **D)** Simulations from modelling the more detailed miR-199a/b-5p chondrogenesis model were shown here. Colour classes follow Figure 5B.

Discussion:

In this paper we performed experimental and computational analyses to better understand the role of miR-199a/b-5p during chondrogenesis. In contrast *to* miR-140, miR-199a and miR-199b are less well studied regulators of chondrogenesis. Previously the *MIR199* family were identified as pro-chondrogenic in mouse mesenchymal C3H10T1/2 cells, reportedly by targeting *SMAD1* (miR-199a-3p) and *JAG1 (*miR-199a/b-5p), respectively [21,22]. Having previously shown the substantial upregulation of miR-199a/b-5p during chondrogenesis, we now show through both loss- and gain of function experiments that *miR-199a/b-5p* also promotes *SOX9, COL2A1* and *ACAN* expression in human MSC chondrogenesis thus enhancing cartilage generation [6]. RNAseq analysis identified key targets of *miR-199a*/*b-5p* including *FZD6*, *ITGA3* and *CAV1*, which were experimentally validated and subsequently incorporated into an *in silico* kinetic model.

miR-199a and miR-199b are vertebrate-specific miRNAs which exhibit an expression pattern associated with mesenchymal tissues and the skeleton [23]. Antisense transcript *Dmn3os* encodes miR199a and miR214 and its deletion in mice causes skeletal defects including short stature and cranial deformity [24]. Similar phenotypic consequences caused by the loss of *DNM3OS* and therefore *MIR199A* and *MIR214* have also been reported in humans [25]. *miR-214* has since been reported to negatively impact on chondrocyte differentiation, through targeting *ATF4* [26]. Thus, our demonstration of the pro-chondrogenic nature of *miR-199a-5p* and *miR-199b-5p* in human MSCs, in addition to the previous demonstration in mouse C3H10T1/2 cells, further supports the role of these miRNAs in chondrogenesis and formation of the skeleton.

We show for the first-time functional evidence for the miR-199b-5p-*CAV1* interaction to occur in human MSCs. Several mechanisms reported in the literature may also support how *miR-199a/b-5p-CAV1* could regulate chondrogenesis, such as the TGFB

triggering phosphorylation of CAV1 via SRC-kinase, and the TGFB pathway which is of great importance in chondrogenesis [20]. In contrast to *CAV1, FZD6 and ITGA3* have been less well studied as miR-199a/b-5p targets, and though, miR-199a-5p-*FZD6* has been predicted previously, our luciferase assays show for the first time that *FZD6* has been validated as a target of *miR-199a-5p-FZD* [22,27]. Previous work by our group has validated *FZD6* as a target of *miR-140-5p*, so it is likely a highly important gene in chondrogenesis. *ITGA3* meanwhile has been found to be a target of *miR-199a-5p* in neck and head cancer cells, and our results confirm this interaction in humans MSCs [28].

The presented model topology (Figure 5A, 5C) was based on our experimental work. The GRNs/ model was initiated with TGFB3, which is used to initiate chondrogenesis and was therefore used as the proxy for chondrogenic initiation. As such, TGFB3 promoted *miR-199a/b-5p* levels to match our microarray data, though based on our previous data TGFB may not directly regulate *miR-199a/b-5p* levels [6]. TGFB3 also induced CAV1 via SRC kinase and induced *SOX9* via the SMAD2-SMAD3 pathway, which then stimulated SOX9 protein production (SMAD2/3 were not included in the models) [29–31]. However, our microarray data showed *CAV1* gene expression decreased during early chondrogenesis, but then increased again – perhaps indicating CAV1 has a smaller negative regulative effect on chondrogenesis, or only effects early chondrogenesis. Gene expression of *FZD6*, *ITGA3*, *CAV1* and the OtherTargets blackbox all had inverse relationships with *miR-199a-5p* and *miR-199b-5p*, and *FZD6* was also negatively regulated by *miR-140-5p*, which we discussed previously [6]. *SOX9* mRNA, SOX9 and P-SOX9 were all treated as separate objects, rather than using our *SOX9* mRNA data as a proxy for total SOX9 activity. P-SOX9 promoted *COL2A1*, *ACAN* and *miR-140-5p* expression. *ACAN* contributed directly, and to the greatest extent, to GAG levels (since most cartilage GAGs are post-translationally added to Aggrecan, the protein product of *ACAN*) which was used as the phenotypic level output for the model and a proxy for chondrogenesis progression [6,32–34]. Precise mechanisms

of how FZD6 and ITGA3 regulated chondrogenesis are unclear, with potentially implicated pathways were included in the larger GRN (Supplementary Figure 1). FZD6 is a transmembrane protein which functions as a receptor for WNT signalling proteins to, most commonly, activate the non-canonical planar cell polarity (PCP) pathway. However, elements of the Wnt signalling pathway have been implicated to act antagonistically to chondrogenesis [35,36]. ITGA3 is a cell surface integrin which forms a heterodimer with ITGB1 to form α3β1 heterodimers through which Chondrocyte-fibronectin ECM connections can be created [37,38]. Conditional deletion of *Itgb1* in cartilage impacts profoundly on skeletogenesis in mice [39]. α3 integrins have been found to increase in OA cartilage, though a direct mechanism between ITGA3 regulating SOX9 is not clear. Regulation of SOX9 via CAV1 has been more studied, which has shown that the relationship between SOX9 and CAV1 is complex and requires further testing. CAV1 may be affecting SOX9 levels, via its activation of RHOA/ROCK1 signalling, which leads to phosphorylation of SOX9, and also RHOA/ROCK1 inhibition has been shown to both increase levels of SOX9 and chondrogenesis biomarkers in mouse ATDC5 cells, but also decrease levels of *SOX9* and chondrogenesis biomarkers in 3D-chondrocytes [30,40–42]. It is likely that other mRNA targets of miR-199a/b-5p also contributed chondrogenesis regulation, such as the other genes identified as miR-199a/b-5p targets from the RNAseq analysis e.g. *MYH9*, *NECTIN2*. Based on this limitation, a “blackbox” called OtherTargets was added to the kinetic model to represent all other anti-chondrogenic *miR-199a/b-5p* targets during chondrogenesis which were not explored in this study.

The complexity of the 199a/b-chondrogenesis system was one of the main reasons for investing in kinetic modelling. To this end, we created a kinetic model based on our experimental work. This is the first kinetic model which contains multiple miRNAs which regulate chondrogenesis.

Conclusion: Our combined bioinformatic, laboratory, and systems biology approach is a novel method to identify and explore both miR-199a-5p and miR-199b-5p as pro-chondrogenic regulators. Based on our bioinformatic analysis, the three most significantly positively changing *miR-199a/b-5p* were predicted targets *FZD6*, *ITGA3* and *CAV1*. Laboratory experiments validated these as direct miR-199a/b-5p targets and confirmed that miR-199a/b-5p positively regulate chondrogenesis. However, the complex nature of miRNA function means there are likely multiple mRNA targets of miR-199a/b-5p which may work synergistically to modulate chondrogenesis. Th e GRN and kinetic models were created to capture the behaviours of the system which act as a useful resource for further experimental design.

Methods:

Data Processing and differential expression analysis. mRNA and miRNA data were produced by Illumina and Exiqon microarray technologies respectively and this is described in *Barter et al (2015)* [6]. mRNA data was processed using the *lumi* R package and the miRNA data was processed using the *affy* R package [43,44]. *limma* was then used to perform pairwise differential expression (DE) analysis [45]. Here the zero-time point was used as the common denominator for all DE analyses. The time point based DE analyses were: D1/D0, D3/D0, D6/D0, D10/D0 and D14/D0. This type of time point based DE analysis was ideal for pair-wise differential expression analysis aproach, as explain by *Spies et al (2019)* [46]. Genes which were significantly differentially expressed (BH adjusted P values <0.05) in at least one of the DE analyses have their adjusted P values and log2FC values were kept for analysis by the *TimiRGeN R* package. All data wrangling and processing took place in *R*.

Analysis with the *TimiRGeN R* package. Dataframes containing mRNA and miRNA DE results are analysed using the combined mode of *TimiRGeN* [11]. The threshold for time point specific gene filtration was set as <0.05 and adjusted P values were used for filtration. Time point specific pathway enrichment used microarray probe IDs as the background dataset. Our data was from microarrays so for more accurate Overrepresentation analysis we required the microarray specific gene lists to use as the background set of genes. GPL10558 (mRNA) and GPL11434 (miRNA) were downloaded from GEO and the probes were annotated with entrezgene IDs using *BiomaRt* [47,48]. Eight signalling pathways were enriched for at least three of the five time point based DE analyses performed. miRNA-mRNA interactions were retained if they had a negative Pearson correlation of < -0.75 and if they were identified two of the three target databases used by *TimiRGeN*.

Human bone marrow MSC culture. Human bone marrow MSCs (from seven donors, 18-25 years of age) were isolated from human bone marrow mononuclear cells (Lonza Biosciences) and cultured and phenotype-tested as described previously [6]. Experiments

were performed using cells between passage 2 and 10, and all experiments were repeated with cells from a minimum of three donors.

Chondrogenic differentiation. MSCs were re-suspended in chondrogenic culture medium consisting of high-glucose DMEM containing 100 µg/ml sodium pyruvate, 10 ng/ml TGFβ3, 100 nM dexamethasone, 1× ITS-1 premix, 40 µg/ml proline and 25 µg/ml ascorbate-2-phosphate. 5×10^5 MSCs in 500 µl chondrogenic medium were pipetted into 15ml falcon tubes or 5×10^4 MSCs in 150 µl chondrogenic medium were pipetted into a UV-sterilised V-bottom 96-well plate, and then centrifuged at 500 g for 5 min. Media were replaced every 2 or 3 days for up to 7 days.

Dimethylmethylene blue assay. Chondrogenic pellets and transwell discs were digested with papain (10 U/ml) at 60°C [49]. The sulphated glycosaminoglycan (GAG) content was measured by 1,9-dimethylmethylene blue (DMB) binding (Sigma) using chondroitin sulphate (Sigma) as standard [50].

RNA and miRNA Extraction and Real-Time Reverse Transcription PCR. MSC chondrogenic pellets were disrupted in Ambion Cells-to-cDNA II Cell Lysis buffer (for real-time RT-PCR) or mirVana miRNA Isolation Kit Phenol (for RNA-seq) (both Life Technologies) using a small disposable plastic pestle and an aliquot of Molecular Grinding Resin (G-Biosciences/Genotech). Total RNA was then extracted and converted to cDNA using MMLV reverse transcriptase (Invitrogen) and TaqMan real-time RT-PCR was performed, and gene expression levels were calculated as described previously [51]. Primer sequences and assay details can be found in Supporting Information Materials. For single miRNA-specific analysis, RNA was reverse-transcribed with Applied Biosystems TaqMan MicroRNA Reverse Transcription Kit (Life Technologies) and real-time RT-PCR performed with TaqMan MicroRNA assays (Life Technologies). All values are presented as the mean ± SEM of replicates in pooled experiments. For experiments with multiple MSC donors statistical testing was performed using a matched paired two-tailed Student's t test on log-transformed values to account for non-normal distribution.

miRNA Mimic/Inhibitor Transfection in MSC. For modulation of *miR-199* levels in MSC, Dharmacon miRIDIAN mimics (C-300607) or miRIDIAN hairpin inhibitors (IH-300607) were transfected into 40%–50% confluent MSC using Dharmafect 1 lipid reagent (Horizon Discovery) at 100 nM final concentration. Analysis was performed in comparison with Dharmacon miRIDIAN miRNA mimic nontargeting Control #2 (CN-002000-01) or Dharmacon miRIDIAN miRNA hairpin inhibitor nontargeting Control #2 (IN-002005-01). For all experiments, cells were subject to a single transfection prior to induction of MSC differentiation.

Cloning and Plasmid Transfection in SW1353 Cells. Full length miRNA target 3'UTRs were amplified from human genomic DNA using PCR primers (Supplementary Table 4) to enable Clontech In-Fusion HD cloning (Takara Bio Europe, Saint-Germain-en-Laye, France) into the pmirGLO Dual-Luciferase miRNA Target Expression Vector (Promega, Southampton, U.K.) following the manufacturer's instructions. Mutation of the miRNA seed-binding sites was performed using the QuikChange II Site-Directed Mutagenesis Kit (Agilent Technologies) (Supplementary Figure 2). All vectors were sequence verified. SW1353 chondrosarcoma cells were plated overnight in 96-well plates at 50% confluence (1.5 x 10^4 cells/cm^2). Cells were first transfected with 3′UTR luciferase constructs (10 ng) using FuGENE HD transfection reagent (Promega) for 4 hours then transfected with Dharmacon *miR-199a-5p* mimic (50 nM) or miRNA mimic nontargeting Control #2 using Dharmafect 1. After 24 hours of transfection, the SW1353 cells were washed and lysed using Reporter Lysis Buffer (Promega) and firefly and renilla luciferase levels determined using the Promega Dual-Luciferase Reporter Assay System and a GloMax 96 Microplate Luminometer (Promega).

RNAseq. RNA isolated as described above was quality assessed with the Agilent Technology 4200 TapeStation system using an RNA screentape assay (Agilent). cDNA libraries were generated using the Illumina TruSeq Stranded mRNA protocol, combinatorial dual index adapters were used to multiplex/pool libraries. Single-read

sequencing, 76 cycles (75+1 cycle for index sequences), on an Illumina NextSeq500 instrument using a high-output 75 cycle kit. *Kallisto* was used for alignment free RNAseq processing [52]. *Tximport* was used to import the RNAseq data into *R* for further processing [53].

RNAseq DE and miRNA target identification. Time-matched MSC miRNA inhibition (miR-199a-5p and miR-199b-5p) and MSC controls were contrasted by DE using *DESeq2* [54]. m*iRNAtap* was used to score and identify all potential mRNA targets of both *miR-199a-5p* and *miR-199b-5p* [16]. Using several target databases, potential mRNA targets were scored and ranked. Low-level scoring miRNA targets (50 or below) and negatively changing genes from the time series dataset were removed, leaving ound 21 genes that were significantly (adjusted P values < 0.05) upregulated during day 0 or day 1 following miR-199a-5p and miR-199b-5p inhibition.

GRN development. The initial system shematic was made on BioRender (Figure 5A). For the enhanced model, we used *CellDesigner*, SMBL style GRNs are created to represent the biological processed of interest [55]. A literature search provided information of GRN topology. Once the whole GRN was created (Figure 5C), a more advanced GRN was created to hypothesise further pathways and important players in the system which could not be modelled as we lacked the experimental data to do so (Supplementary Figure 2).

Kinetic modelling. The validation data (Figure 2, 4) from qPCR data was converted to numbers compatible to the calibration data from the microarrays using the following formula $KD/C * M$, *KD* being the mean miR-199a-5p or miR-199b-5p value, *C* being the mean control value and M being the mean microarray value. The initial conditions (zero time point) for the calibration and validation datasets were assumed to be the same so the model can have a single initial condition for each validated species. Thus, *KD/C =1* was fixed for each zero-time point, for each species where validation data was available. Species selected from the modelled GRN were modelled using *COPASI* [56]. Calibration was performed using parameter estimation via the Particle swarm algorithm.

Inhibition of miR-199a-5p and miR-199b-5p were simulated using events, where the miRNA in question was reduced by 90-95%, until day 7 in the initial model and day 4.5 in the enhanced model. Parameters were altered using sliders to make the model perform miR-199a-5p or miR-199b-5p inhibition behaviour. Mean squared error (MSE) was calculated between actual and simulated data where possible, $1/n \,.\sum_{i=1}^{n}(yi - \hat{y}i)^2$. Model formulas and parameters are in the Supplementary materials. Data from *COPASI* was imported into *R* for plotting.

Data availability

All scripts will be found in the following github directory X. The enhanced kinetic model can be found in the following biomodels repository X. RNAseq data can be made available on request. Experimental data will be in excel files which will be found stored with the supplementary materials.

Funding

K.P., I.M.C., M.J.B. and D.Y. were supported by the Dunhill Medical Trust [R476/0516]. D.P.S. was supported by Novo Nordisk Fonden Challenge Programme: Harnessing the Power of Big Data to Address the Societal Challenge of Aging [NNF17OC0027812]. C.P. and D.Y. were supported by the MRC and Versus Arthritis as part of the Medical Research Council Versus Arthritis Centre for Integrated Research into Musculoskeletal Ageing (CIMA) [MR/P020941/1 and MR/R502182/1]. J.S. received funding from Versus Arthritis [22043].

Acknowledgements

Contributions

All authors provided substantial contributions to conception or design of the study: J.S., D.A.Y. Substantial contributions to drafting the manuscript: K.P, M.J.B., D.S., and

D.A.Y. Substantial contributions to data acquisition: M.J.B. All authors contributed to data analysis or interpretation, but this was predominately driven by K.P., J.S., and M.J.B. All authors contributed to revising the manuscript critically for important intellectual content and approved the final manuscript.

Conflicts of interest. None.

References:

1. Bosnakovski, D. *et al.* Chondrogenic differentiation of bovine bone marrow mesenchymal stem cells (MSCs) in different hydrogels: Influence of collagen type II extracellular matrix on MSC chondrogenesis. *Biotechnol Bioeng* **93**, (2006).
2. Akkiraju, H. & Nohe, A. Role of chondrocytes in cartilage formation, progression of osteoarthritis and cartilage regeneration. *Journal of Developmental Biology* vol. 3 Preprint at https://doi.org/10.3390/jdb3040177 (2015).
3. Hoshi, H. *et al.* Effect of inhibiting MMP13 and ADAMTS5 by intra-articular injection of small interfering RNA in a surgically induced osteoarthritis model of mice. *Cell Tissue Res* **368**, (2017).
4. Grässel, S. & Muschter, D. Recent advances in the treatment of osteoarthritis. *F1000Research* vol. 9 Preprint at https://doi.org/10.12688/f1000research.22115.1 (2020).
5. Loeser, R. F., Goldring, S. R., Scanzello, C. R. & Goldring, M. B. Osteoarthritis: A disease of the joint as an organ. *Arthritis and Rheumatism* vol. 64 Preprint at https://doi.org/10.1002/art.34453 (2012).
6. Barter, M. J. *et al.* Genome-wide microRNA and gene analysis of mesenchymal stem cell chondrogenesis identifies an essential role and multiple targets for miR-140-5p. *Stem Cells* **33**, (2015).
7. Bartel, D. P. MicroRNAs: Target Recognition and Regulatory Functions. *Cell* vol. 136 Preprint at https://doi.org/10.1016/j.cell.2009.01.002 (2009).
8. Sevignani, C., Calin, G. A., Siracusa, L. D. & Croce, C. M. Mammalian microRNAs: A small world for fine-tuning gene expression. *Mammalian Genome* vol. 17 Preprint at https://doi.org/10.1007/s00335-005-0066-3 (2006).
9. Lai, E. C. Micro RNAs are complementary to 3' UTR sequence motifs that mediate negative post-transcriptional regulation. *Nat Genet* **30**, (2002).
10. Doench, J. G. & Sharp, P. A. Specificity of microRNA target selection in translational repression. *Genes Dev* **18**, (2004).
11. Patel, K. *et al.* TimiRGeN : R/Bioconductor package for time series microRNA–mRNA integration and analysis . *Bioinformatics* (2021) doi:10.1093/bioinformatics/btab377.
12. Agarwal, V., Bell, G. W., Nam, J. W. & Bartel, D. P. Predicting effective microRNA target sites in mammalian mRNAs. *Elife* **4**, (2015).
13. Huang, H. Y. *et al.* MiRTarBase 2020: Updates to the experimentally validated microRNA-target interaction database. *Nucleic Acids Res* **48**, (2020).
14. Chen, Y. & Wang, X. MiRDB: An online database for prediction of functional microRNA targets. *Nucleic Acids Res* **48**, (2020).
15. Jin, H. Y. *et al.* Transfection of microRNA mimics should be used with caution. *Front Genet* **6**, (2015).
16. Pajak M & Simpson TI. miRNAtap: microRNA Targets - Aggregated Predictions. Preprint at (2021).
17. Soul, J., Hardingham, T. E., Boot-Handford, R. P. & Schwartz, J. M. Skeletalvis: An exploration and meta-analysis data portal of cross-species skeletal transcriptomics data. *Bioinformatics* **35**, (2019).

18. Huang, A. H., Stein, A. & Mauck, R. L. Evaluation of the complex transcriptional topography of mesenchymal stem cell chondrogenesis for cartilage tissue engineering. *Tissue Eng Part A* **16**, (2010).
19. Huynh, N. P. T., Zhang, B. & Guilak, F. High-depth transcriptomic profiling reveals the temporal gene signature of human mesenchymal stem cells during chondrogenesis. *FASEB Journal* **33**, (2019).
20. Lino Cardenas, C. L. *et al.* miR-199a-5p Is Upregulated during Fibrogenic Response to Tissue Injury and Mediates TGFbeta-Induced Lung Fibroblast Activation by Targeting Caveolin-1. *PLoS Genet* **9**, (2013).
21. Zhang, M. *et al.* miR-199b-5p promoted chondrogenic differentiation of C3H10T1/2 cells by regulating JAG1. *J Tissue Eng Regen Med* **14**, (2020).
22. Lin, E. A., Kong, L., Bai, X. H., Luan, Y. & Liu, C. J. MiR-199a*, a bone morphogenic protein 2-responsive MicroRNA, regulates chondrogenesis via direct targeting to Smad1. *Journal of Biological Chemistry* **284**, 11326–11335 (2009).
23. Desvignes, T., Contreras, A. & Postlethwait, J. H. Evolution of the miR199-214 cluster and vertebrate skeletal development. *RNA Biol* **11**, (2014).
24. Watanabe, T. *et al.* Dnm3os, a non-coding RNA, is required for normal growth and skeletal development in mice. *Developmental Dynamics* **237**, (2008).
25. Lefroy, H., Fox, O., Javaid, M. K., Makaya, T. & Shears, D. J. 1q24 deletion syndrome. Two cases and new insights into genotype-phenotype correlations. *Am J Med Genet A* **176**, (2018).
26. Roberto, V. P. *et al.* Evidences for a New Role of miR-214 in Chondrogenesis. *Sci Rep* **8**, (2018).
27. Kim, B. K., Yoo, H. I., Kim, I., Park, J. & Yoon, S. K. FZD6 expression is negatively regulated by miR-199a-5p in human colorectal cancer. *BMB Rep* **48**, (2015).
28. Tian, L., Chen, M., He, Q., Yan, Q. & Zhai, C. MicroRNA-199a-5p suppresses cell proliferation, migration and invasion by targeting ITGA3 in colorectal cancer. *Mol Med Rep* **22**, (2020).
29. Coricor, G. & Serra, R. TGF-β regulates phosphorylation and stabilization of Sox9 protein in chondrocytes through p38 and Smad dependent mechanisms. *Sci Rep* **6**, (2016).
30. Peng, F. *et al.* TGFβ-induced RhoA activation and fibronectin production in mesangial cells require caveolae. *Am J Physiol Renal Physiol* **295**, (2008).
31. Mishra, R., Zhu, L., Eckert, R. L. & Simonson, M. S. TGF-β-regulated collagen type I accumulation: Role of Src-based signals. *Am J Physiol Cell Physiol* **292**, (2007).
32. Roughley, P. J. & Mort, J. S. The role of aggrecan in normal and osteoarthritic cartilage. *J Exp Orthop* **1**, (2014).
33. Hardingham, T. E. & Fosang, A. J. Proteoglycans: many forms and many functions. *The FASEB Journal* **6**, (1992).
34. Huang, W., Zhou, X., Lefebvre, V. & de Crombrugghe, B. Phosphorylation of SOX9 by Cyclic AMP-Dependent Protein Kinase A Enhances SOX9's Ability To Transactivate a Col2a1 Chondrocyte-Specific Enhancer . *Mol Cell Biol* **20**, (2000).
35. Corda, G. & Sala, A. Non-canonical WNT/PCP signalling in cancer: Fzd6 takes centre stage. *Oncogenesis* vol. 6 Preprint at https://doi.org/10.1038/oncsis.2017.69 (2017).
36. Snelling, S. J. B. *et al.* Dickkopf-3 is upregulated in osteoarthritis and has a

chondroprotective role. *Osteoarthritis Cartilage* **24**, (2016).
37. LaPointe, V. L. S., Verpoorte, A. & Stevens, M. M. The changing integrin expression and a role for integrin β8 in the chondrogenic differentiation of mesenchymal stem cells. *PLoS One* **8**, (2013).
38. Loeser, R. F. Integrins and chondrocyte-matrix interactions in articular cartilage. *Matrix Biology* vol. 39 Preprint at https://doi.org/10.1016/j.matbio.2014.08.007 (2014).
39. Aszodi, A., Hunziker, E. B., Brakebusch, C. & Fässler, R. β1 integrins regulate chondrocyte rotation, G1 progression, and cytokinesis. *Genes Dev* **17**, 2465–2479 (2003).
40. Xu, T., Wu, M., Feng, J., Lin, X. & Gu, Z. RhoA/Rho kinase signaling regulates transforming growth factor-β1-induced chondrogenesis and actin organization of synovium-derived mesenchymal stem cells through interaction with the Smad pathway. *Int J Mol Med* **30**, (2012).
41. Woods, A. & Beier, F. RhoA/ROCK signaling regulates chondrogenesis in a context-dependent manner. *Journal of Biological Chemistry* **281**, (2006).
42. Woods, A., Wang, G. & Beier, F. RhoA/ROCK signaling regulates Sox9 expression and actin organization during chondrogenesis. *Journal of Biological Chemistry* **280**, (2005).
43. Du, P., Kibbe, W. A. & Lin, S. M. lumi: A pipeline for processing Illumina microarray. *Bioinformatics* **24**, (2008).
44. Gautier, L., Cope, L., Bolstad, B. M. & Irizarry, R. A. Affy - Analysis of Affymetrix GeneChip data at the probe level. *Bioinformatics* **20**, (2004).
45. Ritchie, M. E. *et al.* Limma powers differential expression analyses for RNA-sequencing and microarray studies. *Nucleic Acids Res* **43**, (2015).
46. Spies, D., Renz, P. F., Beyer, T. A. & Ciaudo, C. Comparative analysis of differential gene expression tools for RNA sequencing time course data. *Brief Bioinform* **20**, (2019).
47. Durinck, S., Spellman, P. T., Birney, E. & Huber, W. Mapping identifiers for the integration of genomic datasets with the R/ Bioconductor package biomaRt. *Nat Protoc* **4**, (2009).
48. Edgar, R., Domrachev, M. & Lash, A. E. Gene Expression Omnibus: NCBI gene expression and hybridization array data repository. *Nucleic Acids Res* **30**, (2002).
49. Murdoch, A. D. *et al.* Chondrogenic Differentiation of Human Bone Marrow Stem Cells in Transwell Cultures: Generation of Scaffold-Free Cartilage. *Stem Cells* **25**, (2007).
50. Farndale, R. W., Sayers, C. A. & Barrett, A. J. A direct spectrophotometric microassay for sulfated glycosaminoglycans in cartilage cultures. *Connect Tissue Res* **9**, (1982).
51. Barter, M. J. *et al.* HDAC-mediated control of ERK- and PI3K-dependent TGF-β-induced extracellular matrix-regulating genes. *Matrix Biology* **29**, (2010).
52. Bray, N. L., Pimentel, H., Melsted, P. & Pachter, L. Near-optimal probabilistic RNA-seq quantification. *Nat Biotechnol* **34**, (2016).
53. Soneson, C., Love, M. I. & Robinson, M. D. Differential analyses for RNA-seq: transcript-level estimates improve gene-level inferences. *F1000Res* **4**, (2015).
54. Love, M. I., Huber, W. & Anders, S. Moderated estimation of fold change and dispersion for RNA-seq data with DESeq2. *Genome Biol* **15**, (2014).
55. Funahashi, A. *et al.* CellDesigner 3.5: A versatile modeling tool for biochemical networks. *Proceedings of the IEEE* **96**, (2008).
56. Hoops, S. *et al.* COPASI - A COmplex PAthway SImulator. *Bioinformatics* **22**, (2006).